# Interference-Based Reliability and Capacity Analysis for IEEE 802.11 Broadcast Ad-Hoc Networks on the Highway


Zhijuan Li[1,2][a], Xintong Wu[1], Xiaokun Li[1,2,3][b] and Xiaomin Ma[4]

[1]*Department of Computer and Big Data, Heilongjiang University, Harbin 150080, China*

[2]*Postdoctoral Program of Heilongjiang Hengxun Technology Co., Ltd. Harbin 150090, China*

[3] *School of Computer Science and Technology, Harbin Institute of Technology, Harbin 150001, China*

[4]*College of Science and Engineering, Oral Roberts University, Tulsa, OK 74171, U.S.A.*

*lizhijuan@hrbeu.edu.cn, {wuxintong, lixiaokun}@hlju.edu.cn, xma@oru.edu*



Keywords: Vehicular Ad-Hoc Network, CSMA, SINR, Reliability, Capacity.



Abstract: Interference is a critical factor that degrades wireless network performance. In IEEE 802.11 wireless broadcast networks, hidden terminals and concurrent transmissions are the primary sources of interference due to the carrier sense multiple access (CSMA) mechanism. Therefore, analyzing the signal-to-interference-plus-noise ratio (SINR) distribution is essential for evaluating network performance, whose derivation relates to the transmission probabilities of hidden terminals and concurrent transmissions. In this study, we utilize the existing semi-markov process (SMP) model to calculate these transmission probabilities. Subsequently, we employ the Laplace transform to analyze the SINR distribution in IEEE 802.11 broadcast ad-hoc networks on highways. Based on the derived SINR distribution, we further evaluate the reliability and capacity. This approach can be readily extended to two-dimensional (2D) or three-dimensional (3D) scenarios by employing $d$-dimensional ($1 \leq d \leq 3$, $d$D) point process. Experimental results demonstrate that the proposed model achieves high accuracy under small to medium interference ranges. Additionally, the analysis remains highly accurate for receivers within 70 meters, even in scenarios with large interference ranges.




## 1 INTRODUCTION

Vehicular ad-hoc Networks (VANETs), based on IEEE 802.11p/bd, deliver broadcast services for safety-related applications with strict quality of service (QoS) requirements. IEEE 802.11p/bd defines physical and Medium Access Control (MAC) layer specifications, with 802.11bd enhancing physical layer performance as 802.11p's successor. The MAC layer employs the distributed coordination function (DCF), which relies on CSMA for collision avoidance. However, vehicle-to-vehicle (V2V) communication using CSMA suffers from hidden terminal and concurrent collision problems, degrading channel quality and causing packet loss (Yin et al., 2013). Performance evaluation is thus vital for network planning and optimization (Luong et al., 2017; Li et al., 2020). Common reliability metrics include Node-to-Node Packet Reception Probability (PRP) and Packet Reception Ratio (PRR), which measure the probability that a packet is received successfully from different aspects (Ma et al., 2012).

Researchers have built many analytical models to derive reliability metrics of V2V communication. Some models adopted a deterministic distance-based method, and other models adopted the SINR-based method. In models using deterministic distance-based methods, a packet is considered lost if a collision happens during the transmission of the packet (Li et al., 2022). The size of the geometric region that may cause packet collision, such as length, area, volume, etc. needs to be calculated (Zhao et al., 2020). In SINR-based models, a packet transmission is considered successfully received as long as the SINR exceeds the threshold throughout the packet's transmission, even if a collision occurs, reflecting real-world conditions more accurately. Thus, SINR-based model is developed as a more general and accurate model for analyzing the performance of wireless broadcast network compared to the deterministic distance-based model (Li et al., 2022). The critical step in the SINR-based method is deriving the distribution of SINR, namely probability density function (PDF) and cumu-


[a] https://orcid.org/0000-0002-2162-5654
[b] https://orcid.org/0000-0002-6645-6890





Li, Z., Wu, X., Li, X. and Ma, X.
Interference-Based Reliability and Capacity Analysis for IEEE 802.11 Broadcast Ad-Hoc Networks on the Highway.
DOI: 10.5220/0013356400003941



In *Proceedings of the 11th International Conference on Vehicle Technology and Intelligent Transport Systems (VEHITS 2025)*, pages 520-528
ISBN: 978-989-758-745-0; ISSN: 2184-495X

lative distribution function (CDF) of the SINR at the receiver (Zhao et al., 2021a; Ma and Trivedi, 2021).

Stochastic geometry is a powerful tool for analyzing the distribution of SINR. The application of stochastic geometric analysis hinges on calculating the transmission probability of a node under the CSMA mechanism. Most stochastic geometry-based analytical models for evaluating wireless network performance under CSMA use ALOHA as an approximation. This approach has been applied to one-dimensional (1D) VANETs (Błaszczyszyn et al., 2013), intersection VANET (Ni et al., 2015a; Steinmetz et al., 2015; Belmekki et al., 2020; Kimura and Saito, 2022), and general urban road VANET (Kimura et al., 2016). Recently, Kimura *et al.* (Kimura and Saito, 2022) proposed a broadcast rate optimization scheme for intersections using this approach, dividing roads into queuing and running segments to provide closed-form approximations for key performance metrics.

Meanwhile, other stochastic geometry-based models directly analyze CSMA behavior to evaluate SINR distribution and network performance. For example, Nguyen *et al.* (Nguyen et al., 2007) modeled CSMA using a Matérn-II-continuous process, assigning nodes uniformly distributed backoff counters in [0,1]. Tong *et al.* (Tong et al., 2016) improved this by developing a Matérn-II-discrete process to better capture discrete backoff counters and analyze packet transmission success probability in a highway VANETs. They utilized simulation methods to estimate node transmission probabilities. Unlike previous studies that approximated CSMA with ALOHA, their work directly models the CSMA mechanism, providing valuable insights that have inspired our research.

Considering that the SMP model (Yin et al., 2013) characterized the CSMA behavior, the steady-state transmission probability of a node can be calculated. Then the transmission probabilities of hidden terminals and concurrent transmissions during the transmission of the tagged sender can be obtained by the SMP model. On the basis of the SMP model, the probability derivation-based method, the effective interference distance-based method are two other mathematical methods to analyze the SINR distribution of V2V communication in IEEE 802.11 VANET. Zhao *et al.* (Zhao et al., 2021a) built the probability derivation-based method to analyze the performance of VANET at 1D highway by adopting order statistics and non-homogeneous poisson point process (NHPP) distribution and extended the approach to analyze the case of 2D intersections. However, the probability derivation method has high computational complexity and requires parallel computing to solve the SINR distribution, which increases the difficulty of implementation and requires a server with parallel computing power (Zhao et al., 2021a; Zhao et al., 2021b).

In recent years, Ma *et al.* (Ma et al., 2021; Ma and Trivedi, 2021) introduced an efficient interference distance-based method to evaluate reliability metrics such as PRP and PRR by calculating the effective interference range related to the SINR threshold. Building on this, Li *et al.* (Li et al., 2022) refined the model by incorporating a maximum interference range constraint and extended it to analyze the case of 2D intersection VANETs, proposing the SINR-related Effective Distance Constrained by Maximum interference range (SED-CM) model. This model assumes that reception fails if interference occurs within the effective interference range, consistent with deterministic distance-based principles. This approach allows for rapid computation of PRP and PRR by bypassing complex integrals. However, determining link capacity requires numerous time-consuming interpolations, and extending the model to higher dimensions is challenging due to the complexity of computing geometric region sizes (Zhao et al., 2020).

In this paper, we propose applying stochastic geometry methods and the SMP model to compute the SINR distribution. Specifically, we employ the Laplace transform to analyze the SINR distribution, accounting for the effects of hidden terminals and concurrent transmissions. Based on the derived SINR distribution, we further calculate reliability metrics and network capacity. The contributions of the paper are as follows.

1) Firstly, we adopt the stochastic geometry method to derive the SINR distribution at the receiver in V2V communication with CSMA mechanism. We evaluate the interference probability of other nodes by the SMP model which captures the full CSMA behavior.
2) Secondly, based on the obtained SINR distribution, we further derive the reliability metrics PRP, PRR, and link capacity.
3) Thirdly, we conduct a series of experiments to validate the model with NS2 simulation.

The rest of the paper is organized as follows. Section 2 describes the system model, including the communication scenario and interference model. Section 3 gives the analysis of SINR distribution conditioned on the receiving distance. Section 4 presents the reliability metrics PRP, PRR as well as link capacity. Section 5 describes the experimental process and results. Section 6 concludes the paper.

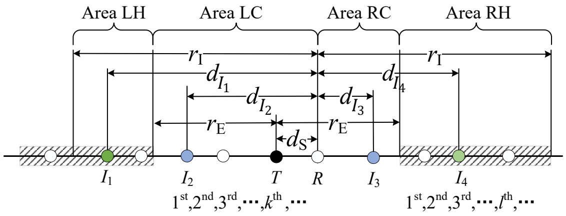


Figure 1: General interfering scenario of IEEE 802.11 broadcast ad-hoc networks on the highway.

## 2 SYSTEM MODEL

In the paper, we consider V2V communication in a highway scenario. As shown in Fig. 1, the highway scenario is abstracted to a 1D line. The number of nodes follows the 1D homogeneous poisson point process (HPPP) with the density $\beta$ (vehs/m). Vehicles periodically broadcast/receive Basic Safety Messages (BSMs) to/from nearby vehicles. $T$ is the tagged sender, $R$ is the tagged receiver. $d_S$ is the distance from the sender $T$ to the receiver $R$. $r_E$ presents the carrier sensing range. $r_I$ is the interference range. We assume signal propagation suffers from *Rayleigh* fading. In this way, the receiving power $P_r$ at a distance $d$ from the sender is:

$$P_r(d) = P_t \eta d^{-\alpha} h \tag{1}$$

where $P_t$ is the transmission power, $\eta = K d_0^{\alpha}$, $K$ is a constant determined by the device, $\alpha$ is the path loss exponent, $d_0$ is the reference distance, and $h$ is a random variable following the exponential distribution with a mean of one. The sensing range can be computed by $r_E = d_0 \sqrt[\alpha]{P_t K / P_{th}}$, $P_{th}$ is the carrier sensing threshold.

During the transmission of $T$'s packet, $R$ can also receive signals sent from other nodes except $T$, reducing the SINR of $T$'s transmission. The expression of SINR is:

$$\mathrm{SINR} = \frac{P_r}{I_\Sigma + N_0} = \frac{P_t \eta d_S^{-\alpha} h}{I_\Sigma + N_0} \tag{2}$$

where $N_0$ is the power of noise, $I_\Sigma$ is the total interference power.

Under the effect of CSMA, the interferers are classified into two classes: concurrent transmissions and hidden terminal (Yin et al., 2013). The hidden terminal area is beyond the sensing range of the tagged sender and within the interference range. The concurrent transmission area is within the sensing range of the tagged sender. Then, we split four interference areas for the receiver $R$: Left Hidden (LH) terminal area, Left Concurrent (LC) transmission area, Right Concurrent (RC) transmission area, and Right Hidden (RH) terminal area, as shown in Fig. 1. The tagged sender $T$ is the origin. Area LH is within the range of $[-r_I + d_S, -r_E]$, area LC is within the range of $[-r_E, d_S]$, area RC is within the range of $[d_S, r_E]$, and area RH is within the range of $[r_E, r_I + d_S]$.

$I_1(I_4)$ represents the interference node in area LH(RH). Assuming that there are $l(l')$ nodes in area LH(RH), $d_{I_1}$ $(I_1 = 1, \cdots, l)(d_{I_4}$ $(I_4 = 1, \cdots, l'))$ denote the distance between the receiver $R$ and the $I_1(I_4)$-th node within area LH(RH). We have $d_S + r_E \leq d_{I_1} \leq r_I$, $r_E - d_S \leq d_{I_4} \leq r_I$.

In the same way, $I_2(I_3)$ represents the interference node in area LC(RC). Assuming that there are $k$ nodes in area LC, $d_{I_2}$ $(I_2 = 1, \cdots, k)(d_{I_3}$ $(I_3 = 1, \cdots, k'))$ denote the distance between the receiver $R$ and the $I_2(I_3)$-th node with area LC(RC). We have $0 \leq d_{I_2} \leq d_S + r_E$ and $0 \leq d_{I_3} \leq r_E - d_S$.

Furthermore, the proportion of nodes in different interference regions contributing to aggregate interference is denoted as: $g_X(X \in [\mathrm{LH}, \mathrm{LC}, \mathrm{RC}, \mathrm{RH}])$. The expression of $g_X$ is as follows.

$$g_X = \begin{cases} \pi_0 & X \in [\mathrm{LC}, \mathrm{RC}] \\ p_t & X \in [\mathrm{LH}, \mathrm{RH}] \end{cases} \tag{3}$$

where $p_t$ presents the hidden terminal transmission probability during the vulnerable period. and $\pi_0$ represents the probability that a neighbor starts to transmit a packet at the beginning of the same time slot with the tagged vehicle. We calculate $p_t$ and $\pi_0$ by solving the steady-state probability $\pi_{\mathrm{XMT}}$ that the node is in the transmitting state in the SMP model (Yin et al., 2013).

## 3 SINR CONDITIONAL DISTRIBUTION ANALYSIS

In the section, we derive the CDF and PDF of SINR at the receiver by utilizing the Laplace transform of overall interference at the receiver.

### 3.1 The CDF and PDF of SINR at the Receiver

As shown in Fig. 1, $T$ is the tagged sender, $R$ is the receiver. $d_S$ is the distance between $T$ and $R$. According to the definition of SINR in (2), the CDF of SINR conditioned on receiving distance $d_S$ is:

$$\begin{aligned} F_{\mathrm{SINR}}(x|d_S) &= P(\mathrm{SINR} \leq x|d_S) \\ &= 1 - P(\mathrm{SINR} > x|d_S) \\ &= 1 - P\left(\frac{P_t \eta h d_S^{-\alpha}}{I_{\mathrm{LH}} + I_{\mathrm{LC}} + I_{\mathrm{RC}} + L_{\mathrm{RH}} + N_0} > x\right) \end{aligned} \tag{4}$$

and the PDF of SINR conditioned on receiving distance $d_S$ is:

$$f_{\text{SINR}}(x|d_S) = \frac{\mathrm{d}F_{\text{SINR}}(x|d_S)}{\mathrm{d}x} \tag{5}$$

In (4), $N_0$ is the noise power. $I_{\text{LH}}(I_{\text{LC}}, I_{\text{RC}}, I_{\text{RH}})$ represent the accumulated interference from area LH (LC,RC,RH) on the receiver, which are given by

$$I_{\text{LH}} = \sum_{I_1 \in \Phi_{\text{LH}}} P_t \eta d_{I_1} h_{I_1};\ I_{\text{LC}} = \sum_{I_2 \in \Phi_{\text{LC}}} P_t \eta d_{I_2} h_{I_2} \tag{6}$$

$$I_{\text{RC}} = \sum_{I_3 \in \Phi_{\text{RC}}} P_t \eta d_{I_3} h_{I_3};\ I_{\text{RH}} = \sum_{I_4 \in \Phi_{\text{RH}}} P_t \eta d_{I_4} h_{I_4} \tag{7}$$

In this way, we can rewrite (4) as

$$\begin{aligned} &F_{\text{SINR}}(x|d_S) = \\ &1 - \mathbb{E}_{I_{\text{LH}}, I_{\text{LC}}, I_{\text{RC}}, I_{\text{RH}}}\left[\Pr\Big(h > \frac{x d_S^{\alpha}}{P_t \eta}(I_{\text{LH}} + I_{\text{LC}} + I_{\text{RC}} \\ &+ I_{\text{RH}} + N_0)\Big)\right] \end{aligned} \tag{8}$$

Due to Rayleigh fading, $h \sim \exp(1)$, let $\Delta = x d_S^{\alpha}$, we get

$$\begin{aligned} &F_{\text{SINR}}(x|d_S) = 1 - \exp\Big(-\frac{\Delta}{P_t \eta} N_0\Big) \\ &\times \mathbb{E}_{I_{\text{LH}}, I_{\text{LC}}, I_{\text{RC}}, I_{RH}}\left[\exp\Big(-\frac{\Delta}{P_t\eta} P_t \eta I_{\text{LH}}\Big)\exp\Big(-\frac{\Delta}{P_t \eta} I_{\text{LC}}\Big)\right. \\ &\left.\exp\Big(-\frac{\Delta}{P_t\eta} I_{\text{RC}}\Big)\exp\Big(-\frac{\Delta}{P_t\eta} I_{\text{RH}}\Big)\right] \end{aligned} \tag{9}$$

and using the independence of hidden terminal and concurrent transmission, we finally have that

$$\begin{aligned} F_{\text{SINR}}(x|d_S) = 1 - \exp\Big(-\frac{\Delta}{P_t \eta} N_0\Big) \mathcal{L}_{I_{\text{LH}}}\Big(\frac{\Delta}{P_t\eta}\Big) \\ \mathcal{L}_{I_{\text{LC}}}\Big(\frac{\Delta}{P_t\eta}\Big) \mathcal{L}_{I_{\text{RC}}}\Big(\frac{\Delta}{P_t\eta}\Big) \mathcal{L}_{I_{\text{RH}}}\Big(\frac{\Delta}{P_t\eta}\Big) \end{aligned} \tag{10}$$

where $\mathcal{L}_{I_X}(\frac{\Delta}{P_t\eta})$ is the Laplace transform of $I_X$, which can be interpreted as follows: the Laplace transform of $I_{\text{LH}}$ is the reduction in the probability that SINR is greater than a given threshold due to interference from area LH; the Laplace transform of $I_{\text{LC}}$ is the reduction in the probability that SINR is greater than a given threshold due to interference area LC; the Laplace transform of $I_{\text{RC}}$ is the reduction in the probability that SINR is greater than a given threshold due to interference area RC; the Laplace transform of $I_{\text{RH}}$ is the reduction in the probability that SINR is greater than a given threshold due to interference area RH; and $\exp\Big(-\frac{\Delta}{P_t\eta} N_0\Big)$ can be regarded as a case without interference.

We are now ready to determine expressions for $\mathcal{L}_{I_{\text{LC}}}(\frac{\Delta}{P_t\eta})$, $\mathcal{L}_{I_{\text{RC}}}(\frac{\Delta}{P_t\eta})$, $\mathcal{L}_{I_{\text{LH}}}(\frac{\Delta}{P_t\eta})$, and $\mathcal{L}_{I_{\text{RH}}}(\frac{\Delta}{P_t\eta})$. We derive $\mathcal{L}_{I_{\text{LC}}}(\frac{\Delta}{P_t\eta})$, $\mathcal{L}_{I_{\text{RC}}}(\frac{\Delta}{P_t\eta})$ by considering the effect of interference from concurrent transmissions. Similarly, we derive $\mathcal{L}_{I_{\text{LH}}}(\frac{\Delta}{P_t\eta})$, $\mathcal{L}_{I_{\text{RH}}}(\frac{\Delta}{P_t\eta})$ by considering the effect of interference from hidden terminals.

## 3.2 Effect of Interference from Concurrent Transmissions

1) First, considering the probability of concurrent transmissions, the Laplace transform of the aggregate interference originating from area LC is given by

$$\begin{aligned} &\mathcal{L}_{I_{\text{LC}}}(\frac{\Delta}{P_t\eta}) = \mathbb{E}\left[\exp(-\frac{\Delta}{P_t\eta} I_{\text{LC}})\right] \\ &= \mathbb{E}\left(\prod_{I_2 \in \Phi_{\text{LC}}} \exp\left(-\frac{\Delta}{P_t\eta} P_t \eta d_{I_2}^{-\alpha} h_{I_2}\right)\right) \\ &\overset{(a)}{=} \mathbb{E}_{\Phi_{\text{LC}}}\left(\prod_{I_2 \in \Phi_{\text{LC}}} \mathbb{E}_h(\exp(-\Delta d_{I_2}^{-\alpha} h_{I_2}))\right) \\ &\overset{(b)}{=} \exp\left(-\int_0^{d_S + r_E} \mathbb{E}_h\left[1 - \exp(-\Delta d_{I_2}^{-\alpha} h)\right] \beta \mathrm{d}d_{I_2}\right) \\ &\overset{(c)}{=} \exp\left(-\beta g_{\text{LC}} \int_0^{d_S + r_E} \Big(1 - \exp(-\Delta d_{I_2}^{-\alpha} h)\Big) \mathrm{d}d_{I_2}\right) \\ &= \exp\left(-\beta \pi_0 \int_0^{d_S + r_E} \Big(1 - \exp(-\Delta d_{I_2}^{-\alpha} h)\Big) \mathrm{d}d_{I_2}\right) \end{aligned} \tag{11}$$

where (a) holds due to the independence of the fading parameters, (b) uses the expression of the probability generating functional (PGFL) for a PPP. (c) holds conditional on $h$.

The integral on the right-hand side of (11) is calculated as

$$\begin{aligned} &\int_0^{d_S + r_E} \Big(1 - \exp(-\Delta d_{I_2}^{-\alpha} h)\Big) \mathrm{d}d_{I_2} \\ &\overset{(e)}{=} \int_0^{(d_S + r_E)^{\alpha}} \left(1 - \exp\left(-\Delta h y^{-1}\right)\right) \delta y^{\delta - 1} \mathrm{d}y \\ &\overset{(f)}{=} \int_{(d_S + r_E)^{-\alpha}}^{\infty} \left(1 - \exp\left(-\Delta h x\right)\right) \delta x^{-\delta - 1} \mathrm{d}x \\ &\overset{(g)}{=} (\exp(-\Delta h x) - 1) x^{-\delta} \Big|_{(d_S + r_E)^{-\alpha}}^{\infty} + \\ &\int_{(d_S + r_E)^{-\alpha}}^{\infty} x^{-\delta} \Delta h \exp\left(-\Delta h x\right) \mathrm{d}x \\ &= (1 - \exp(-\Delta h (d_S + r_E)^{-\alpha}))(d_S + r_E) + \\ &(\Delta h)^{\delta} \Gamma(1 - \delta, (d_S + r_E)^{-\alpha}) \end{aligned} \tag{12}$$

where (e) from the substitution $y \leftarrow d_{I_2}^{\alpha}$, $\delta \overset{\text{def}}{=} 1/\alpha$, (f) from $x \leftarrow y^{-1}$, and (g) from the integration by parts. $\Gamma(a,b) = \int_b^{\infty} u^{a-1} e^{-u} \mathrm{d}u$ represents the upper incomplete Gamma function. With the expectation over $h$, we obtain

$$\mathcal{L}_{I_{\mathrm{LC}}}(\frac{\Delta}{P_t\eta}) = \exp\left(-\beta\pi_0\left[(1-\exp(-\Delta\mathbb{E}(h)(d_{\mathrm{S}}+r_{\mathrm{E}})^{-\alpha}))\right.\right.$$
$$\left.\left.(d_{\mathrm{S}}+r_{\mathrm{E}}) + \Delta^{\delta}\mathbb{E}(h^{\delta})\Gamma(1-\delta,(d_{\mathrm{S}}+r_{\mathrm{E}})^{-\alpha}\right]\right) \tag{13}$$

where $h$ is exponential, $\mathbb{E}(h^{\delta}) = \int_0^{\infty} z^{\delta} e^{-z}\mathrm{d}z = \Gamma(1+\delta)$, and $\mathbb{E}(h) = \int_0^{\infty} z e^{-z}\mathrm{d}z = \Gamma(2)$. After a series of derivations,

$$\mathcal{L}_{I_{\mathrm{LC}}}(\frac{\Delta}{P_t\eta}) = \exp\left(-\beta\pi_0\left[(1-A')(d_{\mathrm{S}}+r_{\mathrm{E}})+\right.\right.$$
$$\left.\left.\Delta^{\delta}\Gamma(1+\delta)\Gamma\left(1-\delta,(d_{\mathrm{S}}+r_{\mathrm{E}})^{-\alpha}\right)\right]\right) \tag{14}$$

where $A' = \exp(-\Delta\Gamma(2)(d_{\mathrm{S}}+r_{\mathrm{E}})^{-\alpha})$.

Substituting $\Delta = xd_{\mathrm{S}}^{\alpha}$ yields the desired result:

$$\mathcal{L}_{I_{\mathrm{LC}}}(\frac{xd_{\mathrm{S}}^{\alpha}}{P_t\eta}) = \exp\left(-\beta\pi_0\left[(1-A)(d_{\mathrm{S}}+r_{\mathrm{E}})+\right.\right.$$
$$\left.\left.(xd_{\mathrm{S}}^{\alpha}\eta)^{\delta}\Gamma(1+\delta)\Gamma\left(1-\delta,(d_{\mathrm{S}}+r_{\mathrm{E}})^{-\alpha}\right)\right]\right) \tag{15}$$

where $A = \exp(-x\Gamma(2)(\frac{d_{\mathrm{S}}}{d_{\mathrm{S}}+r_{\mathrm{E}}})^{-\alpha})$.

2) Similar to the derivation of $\mathcal{L}_{I_{\mathrm{LC}}}(\frac{\Delta}{P_t\eta})$, $I_{\mathrm{LC}}$ in (11) is replaced by $I_{\mathrm{RC}}$, $I_2$ is replaced by $I_3$, the upper limit of the integral is replaced by $r_{\mathrm{E}}-d_{\mathrm{S}}$. After a series of derivations, we can obtain the Laplace transform of the aggregate interference from area RC as follows.

$$\mathcal{L}_{I_{\mathrm{RC}}}(\frac{xd_{\mathrm{S}}^{\alpha}}{P_t\eta}) = \exp\left(-\beta\pi_0\left[(1-B)(r_{\mathrm{E}}-d_{\mathrm{S}})+\right.\right.$$
$$\left.\left.(xd_{\mathrm{S}}^{\alpha}\eta)^{\delta}\Gamma(1+\delta)\Gamma\left(1-\delta,(r_{\mathrm{E}}-d_{\mathrm{S}})^{-\alpha}\right)\right]\right) \tag{16}$$

where $B = \exp(-x\Gamma(2)(\frac{d_{\mathrm{S}}}{r_{\mathrm{E}}-d_{\mathrm{S}}})^{-\alpha})$.

### 3.3 Effect of Interference from Hidden Terminal

1) Similar to the derivation of $\mathcal{L}_{I_{\mathrm{LC}}}(\frac{\Delta}{P_t\eta})$, $I_{\mathrm{LC}}$ in (11) is replaced by $I_{\mathrm{LH}}$, $I_2$ is replaced by $I_1$, $\pi_0$ is replaced by $p_{\mathrm{t}}$. The upper limit and lower limit of the integral are replaced by $r_{\mathrm{I}}$ and $r_{\mathrm{E}}+d_{\mathrm{S}}$, respectively. After a series of derivations, we can obtain the Laplace transform of the aggregate interference from area LH as follows.

$$\mathcal{L}_{I_{\mathrm{LH}}}(\frac{xd_{\mathrm{S}}^{\alpha}}{P_t\eta}) = \exp\left(-\beta p_{\mathrm{t}}\left[(A-1)(d_{\mathrm{S}}+r_{\mathrm{E}})-\right.\right.$$
$$(C-1)r_{\mathrm{I}} + (xd_{\mathrm{S}}^{\alpha}\eta)^{\delta}\Gamma(1+\delta)[\gamma(1-\delta,(d_{\mathrm{S}}+r_{\mathrm{E}})^{-\alpha})-$$
$$\left.\left.\gamma(1-\delta,r_{\mathrm{I}}^{-\alpha})]\right]\right) \tag{17}$$

where $C = \exp(-x\Gamma(2)(\frac{d_{\mathrm{S}}}{r_{\mathrm{I}}})^{-\alpha})$.

2) Similar to the derivation of $\mathcal{L}_{I_{\mathrm{LC}}}(\frac{\Delta}{P_t\eta})$, $I_{\mathrm{LC}}$ in (11) is replaced by $I_{\mathrm{RH}}$, $I_2$ is replaced by $I_4$, $\pi_0$ is replaced by $p_{\mathrm{t}}$. The upper limit and lower limit of the integral are replaced by $r_{\mathrm{I}}$ and $r_{\mathrm{E}}-d_{\mathrm{S}}$, respectively. After a series of derivations, we can obtain the Laplace transform of the aggregate interference from area RH as follows.

$$\mathcal{L}_{I_{\mathrm{RH}}}(\frac{xd_{\mathrm{S}}^{\alpha}}{P_t\eta}) = \exp\left(-\beta p_t\left[(B-1)(d_{\mathrm{S}}+r_{\mathrm{E}})^{d}-\right.\right.$$
$$(C-1)r_{\mathrm{I}}^{d} + (xd_{\mathrm{S}}^{\alpha}\eta)^{\delta}\Gamma(1+\delta)[\gamma(1-\delta,(d_{\mathrm{S}}+r_{\mathrm{E}})^{-\alpha})-$$
$$\left.\left.\gamma(1-\delta,r_{\mathrm{I}}^{-\alpha})]\right]\right) \tag{18}$$

where $B$ is the same as in (16) and $C$ is the same as in (17).

## 4 RELIABILITY AND CAPACITY ANALYSIS

Based on the above analysis of SINR distribution conditioned on the receiving distance, we give the expressions of reliability metrics PRP, PRR, and link capacity.

### 4.1 PRP

PRP refers to the probability that a node within the transmission range of the sender successfully receives a packet. It equals the probability that the SINR of a tagged receiver exceeds a threshold $\theta$, i.e.,

$$\mathrm{PRP}(d_{\mathrm{S}}) = P(\mathrm{SINR} > \theta | d_{\mathrm{S}}) = 1 - F_{\mathrm{SINR}}(\theta | d_{\mathrm{S}}) \tag{19}$$

Then we obtain PRP by substituting $\theta$ for $x$ in (10).

### 4.2 PRR

PRR is defined as the percentage of nodes that successfully receive a packet from the tagged transmitter among the neighbors. PRR could be expressed as a function of PRP, as follows:

$$\mathrm{PRR}(d_{\mathrm{S}}) = \frac{\int_0^{d_{\mathrm{S}}} \beta\mathrm{PRP}(x)\mathrm{d}x}{\beta d_{\mathrm{S}}} = \frac{1}{d_{\mathrm{S}}}\int_0^{d_{\mathrm{S}}} \mathrm{PRP}(x)\mathrm{d}x \tag{20}$$

## 4.3 Link Capacity

### 4.3.1 Unconditional SINR Distribution

The CDF and PDF of SINR unconditioned is:

$$\begin{aligned} f_{\mathrm{SINR}}(x) &= \int_0^{r_{\mathrm{E}}} f_{\mathrm{SINR}|d_{\mathrm{S}}}(x) f_{d_{\mathrm{S}}}(t)\mathrm{d}t \\ F_{\mathrm{SINR}}(x) &= \int_0^{x} f_{\mathrm{SINR}}(t)\mathrm{d}t \end{aligned} \tag{21}$$

where $f_{d_{\mathrm{S}}}(x)$ is the receiving distance distribution. Next we derive $f_{d_{\mathrm{S}}}(x)$ using an order statistic method similar to the derivation process in (Zhao et al., 2021a). The difference is that (Zhao et al., 2021a) assumes that the vehicle position follows the NHPP distribution, while this paper assumes that it follows the HPP distribution.

### 4.3.2 Receiving Distance Distribution

$d_{\mathrm{S}}$ is the distance between $T$ and $R$. Independent random variables $0 \le S_1, S_2, \cdot, S_l \le r_{\mathrm{E}}$ denote unordered distances between $T$ and the nodes in the right sensing region. The cumulative probability distribution $P(S_i \le r)$ is given by Theorem 6.2 in (Trivedi, 2008):

$$\begin{aligned} &F_{S_i}(r) = P(S_i \le r | N(s) = 1) \\ &= \frac{P[N(r) = 1, N(s) - N(r) = 0]}{P[N(s) = 1]} = \frac{r}{r_{\mathrm{E}}}, i = 1, ..., l. \end{aligned} \tag{22}$$

Then the PDF of $S_i$ is:

$$f_{S_i}(r) = \frac{1}{r_{\mathrm{E}}}.0 \le r \le r_{\mathrm{E}}, i = 1, \cdots, l \tag{23}$$

Then according to Theorem 6.2 in (Trivedi, 2008), $d_{S_i}(i = 1, ..., l)$ are the order statistics of the random variables $S_i(i = 1, ..., l)$. Thus, the CDF and PDF of distance $d_{S_i}$ $(0 \le d_{S_i} \le r_{\mathrm{E}})$ can be calculated as

$$\begin{aligned} &F_{d_{S_i}}(\tau) = P(d_{S_i} \le \tau) = \sum_{j=i}^{l} \binom{l}{j} F_{S_i}^{j}(\tau)[1 - F_{S_i}(\tau)]^{l-j}, \\ &f_{d_{S_i}}(\tau) = \frac{\mathrm{d}F_{d_{S_i}}(\tau)}{\mathrm{d}\tau}\ ,\ \ 0 \le \tau \le r_{\mathrm{E}}. \end{aligned} \tag{24}$$

The probability that there are $l$ nodes in the right sensing area is $P[l, (0, r_{\mathrm{E}})] = \frac{(\beta r_{\mathrm{E}})^l e^{-\beta r_{\mathrm{E}}}}{l!}$. Then, the total $d_{\mathrm{S}}$'s PDF can be expressed as

$$f_{d_{\mathrm{S}}}(x) = \sum_{l=1}^{\infty} P[l, (0, r_{\mathrm{E}})] \sum_{i=1}^{l} f_{d_{S_i}}(x) p_i, \tag{25}$$

where $p_i$ is the probability that the receiver $R$ is the $i$-th node within the right sensing area, which is evaluated as $p_i = 1/l(i = 1, ..., l)$. So, the $d_{\mathrm{S}}$'s PDF can be solved as follows.

$$\begin{aligned} f_{d_{\mathrm{S}}}(x) &= \sum_{l=1}^{\infty} P[l, (0, r_{\mathrm{E}})] \sum_{i=1}^{l} f_{d_{S_i}}(x) \frac{1}{l} \\ &= f_{S_i}(x) = \frac{1}{r_{\mathrm{E}}},\ \ 0 \le x \le r_{\mathrm{E}} \end{aligned} \tag{26}$$

### 4.3.3 Link Capacity

The distribution and expectation of the link capacity are given in (Ni et al., 2015b). The CDF of the link capacity is as follows.

$$F_{\mathrm{C}}(x) = P\{W log_2(1 + \mathrm{SINR}) < x\} = F_{\mathrm{SINR}}\left(2^{\frac{x}{W}} - 1\right) \tag{27}$$

where $W$ is the bandwidth, $c$ is the link capacity. The PDF of the link capacity is

$$f_{\mathrm{C}}(x) = \frac{\ln 2}{W} \cdot 2^{\frac{x}{W} - 1} f_{\mathrm{SINR}}(2^{\frac{x}{W} - 1}) \tag{28}$$

# 5 EXPERIMENT

## 5.1 Experiment Settings

We use Matlab programs to compute the proposed analytical model in which inputs are the communication parameters and outputs are the CDF and PDF of SINR as well as the reliability metrics: PRP, PRR, and link capacity. Then we conduct a series of experiments to compare the proposed model with NS2 simulation. In the simulation, we deploy the nodes following HPPP on a circular lane with a length of 10 km with a density of 0.1 vehs/m. The 10 km simulation scenario is large enough to objectively evaluate the impact of the interference. The other communication parameters are set as follows: the data rate $R_{\mathrm{d}}$ is 24 Mbps, the carrier frequency $f$ is 5.9 GHz, the channel bandwidth is 10 MHz, the transmission power $P_{\mathrm{t}}$ is 26 dBm, the carrier sensing threshold $P_{\mathrm{th}}$ is -75 dBm, the mean receiving distance $R_0$ where the average receiving power equals the sensing threshold is 500 m, the power of noise $N_0$ is -99 dBm, the reference distance $d_0$ is 1 m, the transmit gain and the receiver gain are both 1.0, constant $\eta$ is $1.64 \times 10^{-5}$, the size of the competition window $W$ is 16, the path loss exponent $\alpha$ is 2, the DIFS is 58 μs, the packet length is 200 Bytes, the slot time $\sigma$ is 13 μs, the packet generation rate $\lambda$ is 10 Hz.

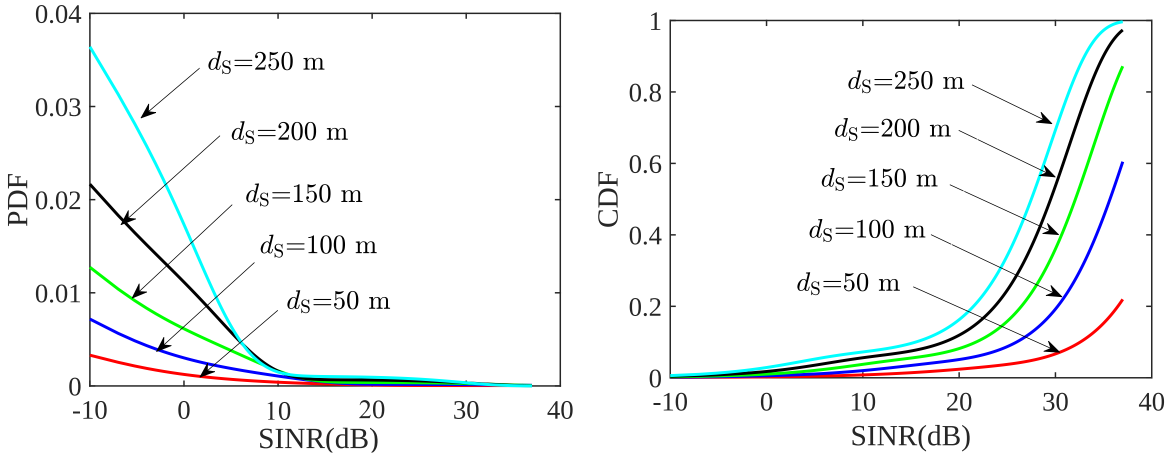


(a) (b)

Figure 2: PDF and CDF of SINR conditioned on the receiving distance $d_S$ while $r_I$ equals 500 m. (a) PDF. (b) CDF.

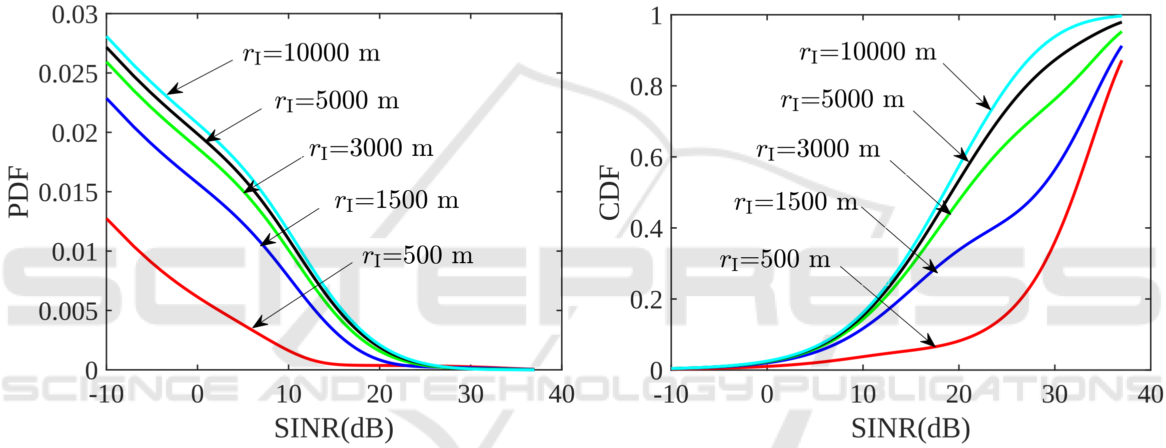


(a) (b)

Figure 3: PDF and CDF of SINR conditioned on the receiving distance of 150 m with different interference range $r_I$. (a) PDF. (b) CDF.



## 5.2 Experiment Results

### 5.2.1 PDF and CDF of SINR

Fig. 2a and Fig. 2b present the PDF and CDF of SINR within 37 dB when the receiving distance $d_S$ equals 50 m, 100 m, 150 m, 200 m, and 250 m, respectively. The minimum interference power is equal to the carrier sensing threshold. In this way, the interference range $r_I$ is equal to the sensing range, which is equal to 500 m. We observe that a smaller receiving distance $d_S$ corresponds to a larger mean of SINR, and otherwise, a larger receiving distance $d_S$ corresponds to a smaller average value of SINR. The reason behind this phenomenon is that the smaller the receiving distance $d_S$, the less power attenuation between the sender and the receiver, resulting in larger receiving power and SINR.

Fig. 3a and Fig. 3b present the PDF and CDF of SINR within 37 dB when the receiving distance $d_S$ equals 150 m, and the interference ranges $r_I$ are set to be 500 m, 1500 m, 3000 m, 5000 m, and 10000 m, respectively. We witness that the greater the interference range, the smaller the mean of SINR. This is expected because more interference would reduce the value of SINR when increasing the interference range. At the same time, we carefully observe the gap between different curves corresponding to $r_I$ and find that the gap is getting smaller and smaller with the increase in the interference range. The phenomenon occurs connecting that the interference power is getting smaller and smaller with the increase in the interference distance due to the effect of the attenuation and path loss of signal propagation. In this way, the distribution of SINR would tend to be stable when the

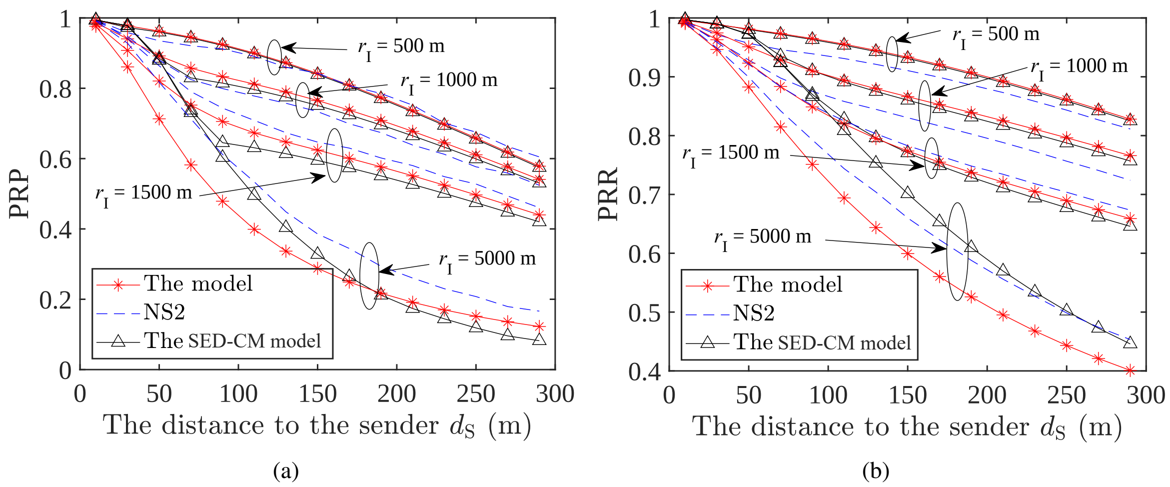


Figure 4: PRP and PRR comparisons between the proposed model, NS2 and the model in (Li et al., 2022), SINR threshold θ = 25 dB. (a) PRPs. (b) PRRs.

interference range reaches a certain level.

#### 5.2.2 PRP and PRR Comparisons

We compute and compare the PRPs and PRRs of the proposed model, NS2 simulation, and the SED-CM model in (Li et al., 2022). PRPs and PRRs at 15 receiving distances are computed with $d_S$ equaling from 10 m to 290 m at an interval of 20 m. The comparison results are shown in Fig. 4 when the density is 0.1 vehs/m, and the SINR threshold θ is equal to 25 dB (corresponding to 316 without dB unit). It can be seen that PRPs and PRRs present decreasing trends with the receiving distance increasing. Because the greater the receiving distance, the smaller the value of SINR, the more packets are lost. Furthermore, we present the results under four interference ranges 500 m, 1000 m, 1500 m, and 5000 m. The results show that the greater the interference range $r_I$, the worse the reliability.

Moreover, we find that PRPs and PRRs of the proposed model are almost in line with the simulation results and the SED-CM results when the interference ranges are 500 m. When the interference ranges are 1000 m and 1500 m, the results show a slight difference in PRPs and PRRs between the proposed model, the NS2 simulation, and the SED-CM model. At the same time, it seems that the results obtained by the proposed model are smoother than the SED-CM model, and have little difference from those of the SED-CM model.

When the interference range is set to 5000 m, the simulation results appear more optimistic than those evaluated by our model, with a larger gap observed between the two. This discrepancy may arise from an overestimation of the hidden terminal's transmission probability at greater distances, leading to an underestimation of successful transmissions. However, we witness that the PRR of the proposed model is almost the same as the NS2 simulation within 70 m, which is the range of interest of emergency since closer interference dominates for close receivers.

Additionally, the SED-CM model applied to $d$D IEEE 802.11 broadcast wireless networks requires calculating the area or volume of irregular regions (Zhao et al., 2020). In contrast, the model proposed in this paper could be adapted to analyze $d$D scenes by utilizing the $d$D point process. We plan to present this work in the future.

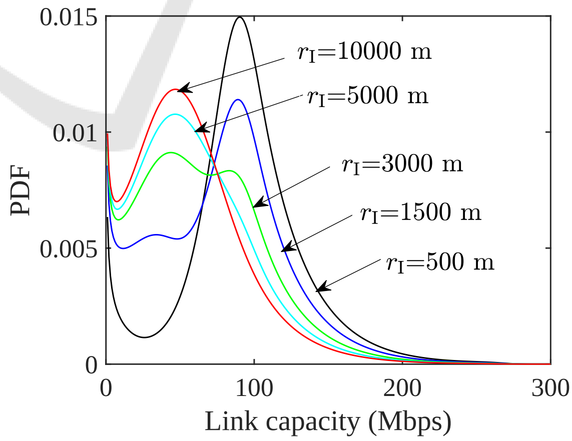


Figure 5: PDF of link capacity.

#### 5.2.3 Link Capacity

Fig. 5 presents the PDF of link capacity in different interference ranges, 500 m, 1500 m, 3000 m, 5000 m, and 10000 m, respectively. These curves present similar changing trends. It could be seen that the mean of link capacity decreases with the increase in the interference range.

# 6 CONCLUSION

The proposed model in the paper uses the stochastic geometry method to evaluate the distribution of SINR, and then derives reliability metrics PRP, PRR, and link capacity of 1D IEEE 802.11 broadcast ad-hoc networks. The experiment results show that the evaluation is accurate for small and medium-distance interference ranges. At the same time, the evaluation is also quite accurate in the closer receivers, even if a larger interference range is assumed. This model can be extended to evaluate the performance of $d$ ($1 \leq d \leq 3$)-dimensional ($d$D) IEEE 802.11 broadcast ad-hoc networks by utilizing a $d$D point process. It is also adaptable to emerging 802.11 technologies, such as orthogonal frequency-division multiple access (OFDMA), multiple input multiple output (MIMO), high-order quadrature amplitude modulation (QAM) ($1024 \sim 4096$), as well as high-frequency and high-bandwidth applications. Future work will focus on exploring these extensions in greater detail.

# ACKNOWLEDGEMENTS

This work is supported by the Basic Scientific Research Funds of Universities of Heilongjiang Province (No. 2023-KYYWF-1485).

# REFERENCES

Belmekki, B. E. Y., Hamza, A., and Escrig, B. (2020). On the outage probability of vehicular communications at intersections over nakagami-m fading channels. In *IEEE 91st VTC Spring*, pages 1–5, Antwerp, Belgium.

Błaszczyszyn, B., Mühlethaler, P., and Toor, Y. (2013). Stochastic analysis of aloha in vehicular ad hoc networks. *Annals of telecommunications-Annales des télécommunications*, 68(1-2):95–106.

Kimura, T. and Saito, H. (2022). Theoretical broadcast rate optimization for v2v communications at intersection. *IEEE Transactions on Mobile Computing*, 21(9):3360–3372.

Kimura, T., Saito, H., Honda, H., and Kawahara, R. (2016). Modeling urban its communication via stochastic geometry approach. In *2016 IEEE 84th Vehicular Technology Conference (VTC-Fall)*, pages 1–5.

Li, W., Song, W., Lu, Q., and Yue, C. (2020). Reliable congestion control mechanism for safety applications in urban vanets. *Ad Hoc Networks*, 98:102033.

Li, Z., Wang, Y., and Zhao, J. (2022). Reliability Evaluation of IEEE 802.11p Broadcast Ad Hoc Networks on the Highway. *IEEE Transactions on Vehicular Technology*, 71(7):7428–7444.

Luong, H. P., Panda, M., Vu, H. L., and Vo, B. Q. (2017). Beacon rate optimization for vehicular safety applications in highway scenarios. *IEEE Transactions on Vehicular Technology*, 67(1):524–536.

Ma, X. and Trivedi, K. S. (2021). SINR-Based analysis of IEEE 802.11p/bd broadcast vanets for safety services. *IEEE Transactions On Network And Service Management*, 18(3):2672–2686.

Ma, X., Yin, X., and Trivedi, K. S. (2012). On the reliability of safety applications in vanets. *International Journal of Performability Engineering*, 8(2).

Ma, X., Zhao, J., Wang, Y., Zhang, T., and Li, Z. (2021). A new approach to sinr-based reliability analysis of ieee 802.11 broadcast ad hoc networks. *IEEE Communications Letters*, 25(2):651–655.

Nguyen, H. Q., Baccelli, F., and Kofman, D. (2007). A stochastic geometry analysis of dense IEEE 802.11 networks. In *Proc. 26th IEEE INFOCOM 2007*, pages 1199–1207, Barcelona, Spain.

Ni, M., Hu, M., Wang, Z., and Zhong, Z. (2015a). Packet reception probability of vanets in urban intersecton scenario. In *Proc. Int. Conf. on Connected Vehicles and Expo*, pages 124–125, Shenzhen, China.

Ni, M., Pan, J., Cai, L., Yu, J., Wu, H., and Zhong, Z. (2015b). Interference-based capacity analysis for vehicular ad hoc networks. *IEEE Communications Letters*, 19(4):621–624.

Steinmetz, E., Wildemeersch, M., Quek, T. Q. S., and Wymeersch, H. (2015). A stochastic geometry model for vehicular communication near intersections. In *2015 IEEE Globecom Workshops (GC Wkshps)*, pages 1–6.

Tong, Z., Lu, H., Haenggi, M., and Poellabauer, C. (2016). A stochastic geometry approach to the modeling of DSRC for vehicular safety communication. *IEEE Transactions on Intelligent Transportation Systems*, 17(5):1448–1458.

Trivedi, K. S. (2008). *Probability & statistics with reliability, queuing and computer science applications*. John Wiley & Sons.

Yin, X., Ma, X., and Trivedi, K. S. (2013). An interacting stochastic models approach for the performance evaluation of DSRC vehicular safety communication. *IEEE Transactions on Computers*, 62(5):873–885.

Zhao, J., Li, Z., Wang, Y., Wu, Z., Ma, X., and Zhao, Y. (2020). An analytical framework for reliability evaluation of d-dimensional IEEE 802.11 broadcast wireless networks. *Wireless Networks*, 26:3373–3394.

Zhao, J., Wang, Y., Lu, H., Li, Z., and Ma, X. (2021a). Interference-based qos and capacity analysis of vanets for safety applications. *IEEE Transactions on Vehicular Technology*, 70(3):2448–2464.

Zhao, J., Zhou, H., Wang, Y., Lu, H., Li, Z., and Ma, X. (2021b). Accelerating interference-based qos analysis of vehicular ad hoc networks for bsm safety applications: Parallel numerical solutions and simulations. In *VEHITS*, pages 600–610.